

Theoretical and experimental photodegradation of Phosmet *via* oxidation techniques in the presence of aqueous TiO₂ suspension

B. Eren¹, Y. Y. Gurkan^{2*}

¹Tekirdag Namik Kemal University, Faculty of Agriculture, Tekirdag, Turkey

²Tekirdag Namik Kemal University, Department of Chemistry, Tekirdag, Turkey

Accepted: November 13, 2021

This study is conducted with the aim to analyze the reaction kinetics of Phosmet with the OH radical, and to determine its mechanism. Due to the lack of experimental evidence of radical intermediate products occurring during the reactions, the theoretical stage has been quite informative. In this study, in order to theoretically determine all probable reaction paths, geometric optimization of the reactants and transition state complexes was conducted using DFT/B3LYP/6-31G(d) basic set of Quantum Mechanical Density Functional Theory (DFT). As a result of the calculations, the energy values at ground state, and rate constant and activation energies (E_a) at transition state (TS) of the probable reaction paths were determined. And finally, the primary intermediate products were found out by the determination of the atom where the OH radicals attach, and the hydrogen atoms they had removed. The reaction mechanism was clarified through the determination of the intermediate products. Since the reactions of pesticides with OH radical are important both in terms of water purification and atmospheric chemistry, the calculations were carried out in gaseous phase and also at aqueous phase by modelling the solvent impact. In the experimental stage, the degradation reactions under UV-light impact of the pesticide, chosen as pollutant, in aqueous TiO₂ suspensions, were analyzed. At the end of this research, the optimum photocatalyst amount and TiO₂ concentration were determined. The degradation rates were determined, the impact of the initial concentration was analyzed, and the reaction products were identified.

Keywords: Phosmet, DFT, Heterogeneous catalysis, Aqueous TiO₂, TS.

INTRODUCTION

There is increasing need for pesticides due to the increasing population in the world. Due to the considerable toxicity of these substances, they require their amount to be traced in nature. Pesticides cause acute and chronic poisoning, also lead to cancer, allergic reactions, damage of the nervous system, learning disability and memory loss, and additionally, cause disorder in enzyme balance as well as damage and mutation in intracellular DNA molecules [1, 2].

Organophosphorus compounds are widely used as pesticides, and these substances react with the OH radical, which is one of the atmospheric radicals, by reaching the atmosphere. The durability of organophosphorus pesticides (OPs) in the nature is short due to their fast decomposition. These pesticides degrade fast; therefore, they do not cause long-term damage. However, they are considerably poisonous. In addition to killing non-targeted insects, these pesticides harm both human and nature. In addition, since they do not have a stable structure, they are applied over and over, and therefore, they are considered as costly [3-10].

Phosmet is an organic compound, and it is known that organic pollutants are present in water at low concentrations. Biomolecules, which are hydroxyl scavengers at different rates, are specific detectors for hydroxyl radicals due to their hydroxylation capability. Any hydroxyl radical attacking an aromatic compound leads to a formation of a hydroxylated new product, and these new products may be more harmful than the original product at the beginning of this process. Therefore, it is essential that these products be observed [11].

Recently, the removal of organic residues using advanced oxidation processes has been observed for water purification technologies. Basically, photocatalytic processes, using semiconductors, which can produce reactive hydroxyl radicals when exposed to UV-radiation, were analyzed in detail [12-14]. Photocatalytic oxidation is one of the advanced technologies in the removal of pollutants due to its effectiveness in the mineralization of organic pollutants [15]. TiO₂ is the most commonly used photocatalysts among others, because it is obtainable, cheap, non-toxic, and has a relatively high chemical stability [16]. TiO₂ is used successfully for the degradation of pesticides [17-19].

* To whom all correspondence should be sent:

E-mail: yyalcin@nku.edu.tr

Phosmet, which is used as OP1 abbreviation in the study, is an organophosphate insecticide used on plants and animals. While it is used mainly for the control of larvae of codling moth on apple trees, it is also used on various fruit plants, ornamental plants, and grapes for the control of suckers, acari, and aphids [20, 21], while it is also used in veterinary fields in the control of pigswill [22]. OP1, which is used as an insecticide and acaricide, is an offensive smelling, off-white crystalline solid [23]. Its melting point is 72-72.7 °C, and decomposes below its boiling point. Its water solubility at 25 °C is 25 mg/L [24] while it is stable at normal storage conditions [25], it is relatively stable at acidic conditions, and decomposes rapidly above 100° C [26]. When heated, it releases extremely toxic fumes such as nitrogen oxide, phosphorous oxide, sulfur oxide [27]. It also has an abrasive effect on metals [28].

METHODOLOGY

In order to theoretically determine all the possible reaction paths of OP1, geometric optimizations were done using the DFT/B3LYP/6-31G(d) basic set of Quantum Mechanical Density Functional Theory (DFT). Energy values were calculated and geometric optimizations were done at all molecular orbital calculations using Gauss View 5.0.8 molecular visualization program and Gaussian 09 program [29]. The energy of decomposition reactions of all organic compounds is affected by the water molecules in aqueous environments. In addition, geometric flexion in solutions is induced by H₂O. In other words, the presence of a dielectric environment such as H₂O leads to a relaxation in geometry, and this situation has an energy reducing, and stabilizing effect [11]. Therefore, in order to explain the solvent effect of H₂O on OP1 + ·OH reaction energy, CPSCM set of COSMO (conductor-like screening solvation model) within the Gaussian 09 packaged software was used. The rate constants and activation energies of the analysed reactions were found out using Transition State Theory (TS) [29]. TS is based on the principle that an equilibrium exists between the reactants in a reaction and the transition state complex. The following equations are used in order to calculate the transition state complexes: E_a activation energies and k constant of OP1 for h = 6.62607 × 10⁻³⁴ J × s, R = 1.987 cal × mol⁻¹ × K⁻¹, T = 298 K and k_B = 1.38.10⁻²³ J × K⁻¹; E_a = E_{TS} - (E_{initial molecule} + E_{OH}) × 627.509 kcal/mol

$$k = \frac{k_B \cdot T}{h} \cdot \frac{Q_{TS}}{Q_{\text{initial molecule}} \times Q_{OH}} \cdot e^{\frac{-E_a}{R \cdot T}}$$

As an experimental method, a stock solution of 10⁻² M of Phosmet was prepared. In the experimental stage, white-coloured, solid, Sigma Aldrich branded Phosmet product number 36195 with a melting point of 73 °C was used. In order to prepare the reaction solution, the determined amount of TiO₂ was weighed and put in the reaction vessel, and the suspension was prepared by adding distilled water. In the experiments, Sigma-Aldrich brand, number 13463-67-7 CAS, odourless, white, TiO₂ powder insoluble in water at 25 °C was used. In order to prepare a good suspension, the reaction vessel was shaken for 15 min in an ultrasonic bath. The organic pollutant concentration was adjusted to be 10⁻⁴ M by adding the stock solution onto this suspension, and the suspension volume was completed to 600 mL. Samples of 10 mL were taken from the prepared suspensions with a pipette, and the rest was placed into a photoreactor in order to be illuminated. A special cylindrical Keriman UV18/8 branded reactor was used in the experiments. As a light source, there were 18 8W UV fluorescent lamps at equal intervals within the cylinder. All experiments were carried out in a Pyrex beaker. The homogenous distribution of TiO₂ particles was provided by shaking the beaker used as a reaction vessel. Since the normal filtration process was not sufficient, samples were filtered in vacuum using 0.2 µm filter-paper in order to remove the TiO₂ particles from the environment. The filtrates were taken into test tubes, and their absorbance was measured on a UV-visible spectrophotometer (Perkin Elmer) at a previously found λ_{max} = 318 nm.

RESULTS AND DISCUSSION

Theoretical Findings for the Ground State

Organophosphorus insecticides are esters of phosphoric acid (H₃PO₄) as a chemical structure. Phosphorus (P) atom is mostly attached to methoxy (OCH₃) or ethoxy (OC₂H₅) as two ester groups. Two methoxy ester groups in the OP1 molecule are seen in Figure 1. The third ester group can be an aliphatic, homocyclic or heterocyclic structure and is attached to the phosphorus atom by ester (P-O-R) or thioester (P-S-R) bonds. This weak bond increases the electrophilicity of the phosphorus atom and gives it electron withdrawing property. In the OP1 molecule, there is a P=S bond instead of P=O, and since two oxygen and two sulfur atoms are attached, the molecule is called dithiophosphate.

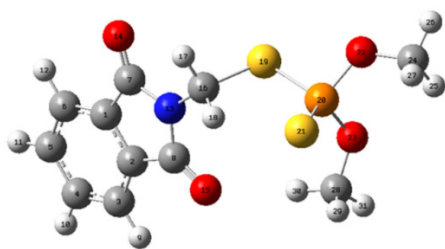


Figure 1. The optimized geometric structure of OP1 via DFT method. (Grey, C; white, H; blue, N; red, O; yellow, S; orange, P)

When the Mulliken loads of the OP1 molecule in Table 1 are analysed, the electronegative atoms are N₁₃, O₂₃, O₂₂, O₁₅, O₁₄, S₂₁, respectively. As it can be seen in Figure 1, O₁₄ and O₁₅ of these atoms form a double bond with C₇ and C₈ atoms. Since these bonds are stable, the bonds are not expected to break. O₂₃, O₂₂ atoms are the second and third electronegative atoms.

Bond lengths of O₂₂-C₂₄ and O₂₃-C₂₈ in Table 2 are 1.44291 Å; 1.44322 Å, respectively, and the bond angle of P₂₀O₂₂C₂₄ is 119.67251°, while the bond angle of P₂₀O₂₃C₂₈ is the third widest bond angle with 121.09768°. Based on this information, it is expected that the methyl groups of C₂₄ and C₂₈ atoms will break. So it is understood that this is the first stage of degradation mechanism N₁₃ is the most electronegative atom. Looking at the area surrounded by this atom; in Table 2, N₁₃-C₁₆ with a bond length of 1.43704 Å, although the N atom is the most electronegative atom, since there are bonds longer than this bond length, it is predicted that if there is a bond break here, it will happen after the other bonds. Even the fact that the bond angles C₈N₁₃C₁₆ and C₇N₁₃C₁₆ in Table 2 have the widest bond angles with 124.831020; 123.050860 respectively, this will not change the situation.

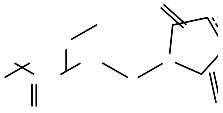
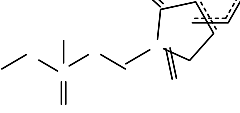
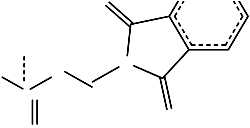
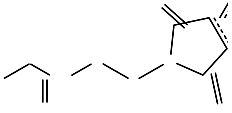
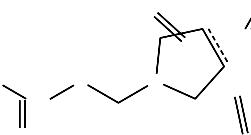
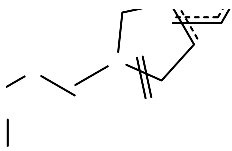
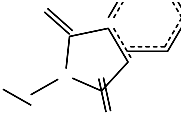
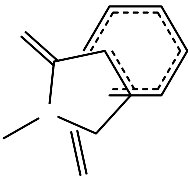
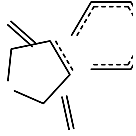
Table 1. Energy values of OP1 in gaseous and aqueous phases, and their Mulliken loads in gaseous phase.

(OP1)Phosmet (C ₁₁ H ₁₂ NO ₄ PS ₂)	Gaseous Phase (kcal × mol ⁻¹)	Aqueous Phase (kcal × mol ⁻¹)	Mulliken Loads
	ΔE= -1919.615320	-1919.629150	C ₃ -0.009525
	ΔH= -1919.614376	-1919.628206	C ₆ -0.006066
	ΔG= -1919.685580	-1919.701667	N ₁₃ -0.511680
			O ₁₄ -0.466116
			O ₁₅ -0.476781
			S ₁₉ 0.001346
			P ₂₀ 0.752968
			S ₂₁ -0.357536
		O ₂₂ -0.497179	
		O ₂₃ -0.504260	

Table 2. Bond lengths and bond angles of atoms of the OP1 molecule.

	Bond Length	(Å)	Bond Angle	(°)
OP1	O ₂₂ -C ₂₄	1.44291	C ₂₄ O ₂₂ P ₂₀	119.67251
	O ₂₃ -C ₂₉	1.44322	O ₂₂ P ₂₀ S ₁₉	95.84725
	P ₂₀ -O ₂₃	1.62316	O ₂₃ P ₂₀ S ₂₁	115.24231
	P ₂₀ -S ₂₁	1.94862	S ₁₉ P ₂₀ S ₂₁	117.55240
	P ₂₀ -S ₁₉	2.12454	O ₂₃ P ₂₀ S ₁₉	107.49501
	C ₁₆ -S ₁₉	1.86489	P ₂₀ S ₁₉ C ₁₆	102.77144
	C ₁₆ -N ₁₃	1.43704	P ₂₀ C ₁₆ N ₁₃	112.40431

Table 3. Energy values in gaseous phase of fragments of OP1 molecule at ground state.

Fragments	Gaseous Phase (kcal/mol)	Fragments	Gaseous Phase (kcal/mol)
 OP1	$\Delta E = -1,204,575.890$ $\Delta H = -1,204,575.297$ $\Delta G = -1,204,619.979$	 OP11	-1,179,928.733 -1,179,928.141 -1,179,971.732
 OP12	-1,155,290.148 -1,155,289.556 -1,155,328.230	 OP13	-1,132,713.373 -1,132,712.780 -1,132,753.264
 OP14	-1,108,069.620 -1,108,069.028 -1,108,106.729	 OP15	-1,060,850.034 -1,060,849.441 -1,060,886.944
 OP16	-596,407.784 -596,407.191 -596,438.267	 OP17	-346,545.368 -346,544.775 -346,572.369
 OP18	-321,892.733 -321,892.140 -321,918.274		

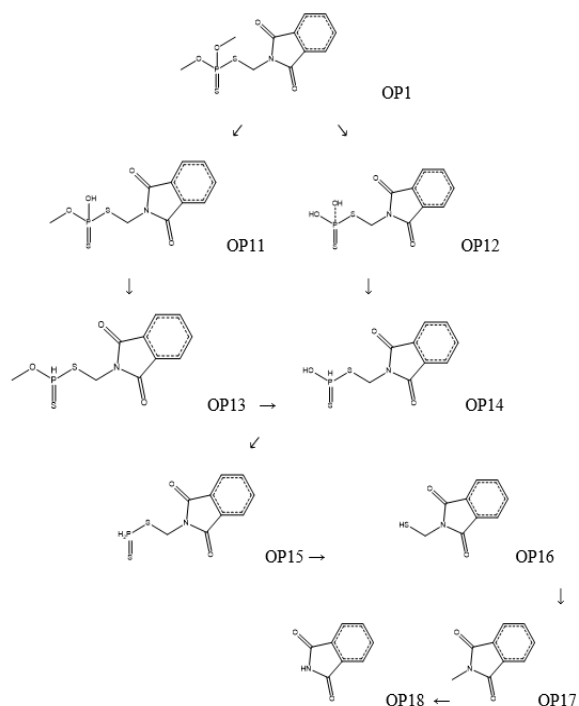


Figure 2. The degradation mechanism of OP1 molecule at ground state.

For the fragments in Table 3, the energy values in the gaseous phase were examined. The lowest energy level, in other words the degradation path starting from the most stable fragment for OP1 in Figure 2, was determined both in the light of the above mentioned predictions, and by the analysis of the energy values of each fragment in Table 3.

Theoretical Findings for the Transition State Complexes

Reactants were used in this study in order to find out the transition state complexes. An appropriate initial geometry estimation was made according to the reaction paths by using the optimum geometric parameters. Transition position complexes were modelled for the reactions that occur with OH addition and H removal. While modeling, C-O bond was chosen as the reaction coordinate. During the calculations, the length of this bond was varied between 1,400-3,000 Å.

As the reaction path; the distance of the forming H₂O molecule, and the length of the bond of OH were chosen, and the dihedral angles and bond lengths related to this group were changed during calculations in order to determine the place of the OH radical according to the molecule. OP1_{TS1} and OP1_{TS2} transition state complexes are obtained *via* OH radical approach with TS to C₃ and C₄ atoms in the benzene ring, and OH bonding to C₃ and C₄ atoms in OP1 molecule. OP1_{TS3} transition position complex is obtained by removing the H atom with

TS from the C₁₆ atom in the OP1 molecule and forming the H₂O molecule. When the OH radical approaches to the C₂₄ and C₂₈ atoms in the OP1 molecule, the OP1_{TS4} transition position complex is obtained by removing the H from the methyl group of the C₂₈ atom and separating a H₂O molecule. All of these transition positions are shown in Figure 3.

The H atom is broken off from the methyl groups at the ends of the molecule and the H₂O molecule is separated, thus, radical formations are realized. This takes place faster than the removal of H atoms from the methyl groups attached to the closed ring or the removal of H atoms from the methyl groups in the intermediate region of the molecule. Attachment of the OH radical to the closed ring takes place at the last step. To clarify this order of velocity, C-OH and C...H₂O bond lengths are given in Table 4. It is seen that the molecule with the longest bond length reacts faster.

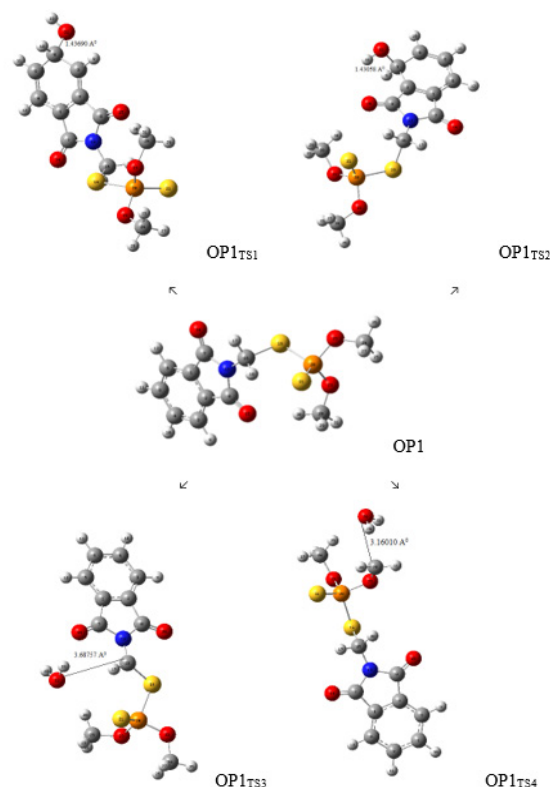


Figure 3. Optimized geometric structures of four possible TS approximations of the OP1 molecule. (Grey, C; white, H; blue, N; red, O; yellow, S; orange, P)

Experimental Findings

Impact of Photocatalyst Concentration. In order to determine the impact of photocatalyst concentration, the TiO₂ concentration was changed as (0.1- 0.5) g/100 mL in suspensions with an initial concentration of 1.0×10⁻⁴ mol L⁻¹ at the natural pH of all substances. The obtained results are given in Figure 4; degradation % for 30, 60, and 90 min,

respectively, at the y axis; and TiO₂ values of (0.1-0.5) g/100 mL at the x axis.

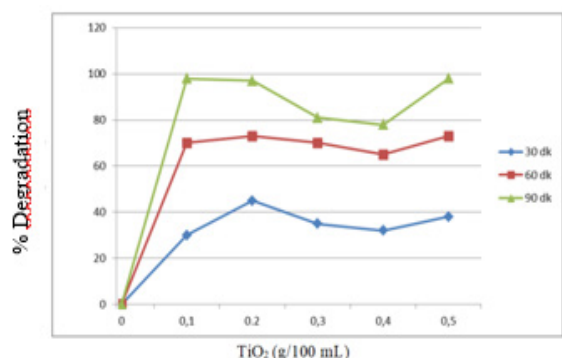


Figure 4. Optimum photocatalytic degradation.

As the TiO₂ concentration increased, the photocatalytic degradation rate increased up to a specific limit of concentration, and then showed a slow decrease. Maximum degradation was obtained at 0.2 g/100 mL of TiO₂ concentration, and this concentration was taken as optimum photocatalyst concentration in all experiments. After the 0.2 g/100 mL optimum value in Figure 4, it was found out that there were other factors getting involved in the degradation rate. As TiO₂ concentration increases, the interparticle distance decreases. Particles form groups by coming together, and this leads to the reduction of the interphase surface. Since organic matters are oxidized on TiO₂ surface by their .OH, the reduction of the interphase surface reduces the possibility of the oxidation of substances; in other words, it reduces the possibility of fragmentation into smaller substances. Moreover, TiO₂ particles prevent the system from absorbing light, and even lead to light scattering.

Impact of Light and Photocatalyst

In order to conduct the degradation of organic matters in heterogeneous photocatalytic degradation systems, the three factors, namely light-semiconductor-O₂, have to be altogether present in the system. Pretestings were conducted in order to determine the impact of light alone on the degradation of substances, and the absorption on

TiO₂ particle surface for the substance. These experiments were conducted in the presence of light only, in TiO₂ presence only, and in the presence of TiO₂+light as three repetitions. The results of these experiments are given in Figure 5. The figure shows the change of C/C₀ against time (t). C₀ is taken as the initial concentration of the substance, whereas C shows the concentration of the substance in t time.

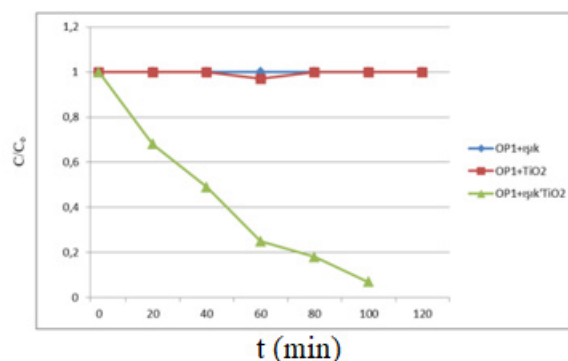


Figure 5. Effect of light and TiO₂ on the photocatalytic degradation of OP1.

As seen in Figure 5, when the change of C/C₀ against time is analyzed, it can be seen that there was no concentration change when OP1 was illuminated (exposed to light) alone. However, when OP1 was kept in the dark together with TiO₂, a slight change in the concentration was observed due to absorption. When OP1 was present in an environment together with both light and TiO₂, it was found out that OP1 was degraded to a great extent. The concentration change at the end of 100 min was found out to be 93%.

Impact of the Initial Concentration

It was analyzed whether the initial concentration had an impact on the photocatalytic degradation rate by changing the initial concentration as (6.0-14.0) × 10⁻⁵ mol L⁻¹. The k rate constants, and r regression values are given in Table 5. The reaction rate constant decreases as the initial concentration increases. However, this decrease declines at lower concentrations.

Table 4. Q values, E_a activation energies, and k rate constants of the studied molecules

Molecule	E _a (kcal × mol ⁻¹)	k	C-OH (Å)	C...H ₂ O (Å)
OP1 _{TS1}	18.578	6.017×10 ⁻⁸	1.43690 (benzene)	
OP1 _{TS2}	19.920	9.199×10 ⁻⁹	1.43058 (benzene)	
OP1 _{TS3}	23.528	3.818×10 ⁻¹⁰		3.68757(intermediate region)
OP1 _{TS4}	13.466	0.049		3.16010 (at the end)

Table 5. Impact of the initial concentration.

OP1	6.0×10^{-5}	8.0×10^{-5}	10.0×10^{-5}	12.0×10^{-5}	14.0×10^{-5}
$k/10^{-18} \text{ min}^{-1}$	2.45 ± 0.002	2.13 ± 0.003	1.76 ± 0.001	1.58 ± 0.004	0.99 ± 0.005
r	0.9885	0.9748	0.9526	0.996	0.9874

The results of the experiments are given in Figure 6. The Figure shows the e-base logarithm, and the change of $\ln C$ according to time for different initial concentrations of organic matter concentrations. The reaction rate constant decreases as the initial concentration increases. However, this decrease declines at low concentrations. Due to the reaction rate constant k being dependent on the initial concentration, it can be said that the degradation reaction is apparently a first-order reaction.

The system consists of two phases. OH radicals result from the OH^- ions absorbed at the TiO_2 surface. Since the organic substance also wants to be absorbed at the TiO_2 surface, it slows down the formation of OH radicals by impeding the transition of OH^- ions into the catalytic space at the surface.

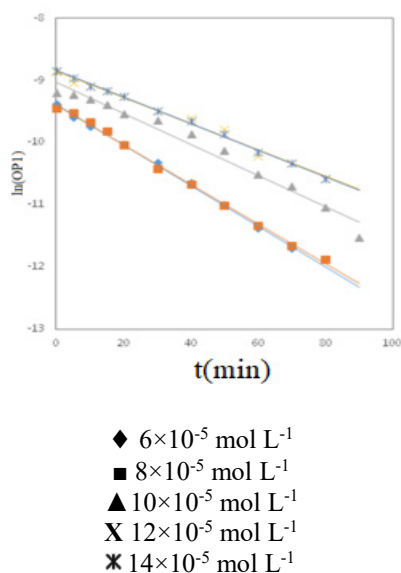


Figure 6. The impact of the initial concentration of OP1 on the photocatalytic degradation rate.

CONCLUSIONS

This research was conducted both theoretically and experimentally by the use of Phosmet (OP1), which was part of a study carried out with seven pesticides comprising four organophosphorus, and three carbamate pesticides. The photocatalytic degradation of OP1 was investigated in aqueous TiO_2 suspensions with UV light. The best degradation rate was obtained at $10 \times 10^{-5} \text{ mol L}^{-1}$ initial concentration with UV/ TiO_2 . Experimental results indicated that the maximum degradation of OP1 occurred at 0.2 g/100 mL TiO_2 concentration. Based on the results of DFT calculations, weakly

bonded pre-reactive complexes were important for the degradation reactions because they were reducing the energy barrier.

Radical formation through the H atom being broken off from the methyl groups at the ends of the molecule and the H_2O molecule being separated takes place faster than the removal of H atoms from the methyl groups attached to the closed ring or the removal of H atoms from the methyl groups in the intermediate region of the molecule. In conclusion, the degradation pathway at ground state of Phosmet molecule, as given in Figure 2, and all the transition positions, as given in Figure 3, clarify the degradation mechanism of Phosmet molecule in the nature in terms of atmospheric and aqueous chemistry.

REFERENCES

- G. Dolapsakis, I. G. Vlachonikolis, C. Varveris, A. M. Tsatsakis, *European Journal of Cancer*, **37**, 1531 (2001).
- L. Sarabia, I. Maurer, E. Bustos Obregon, *Ecotoxicology and Environmental Safety*, **72**, 938 (2009).
- R. Atkinson, S. M. Aschmann, M. A. Goodman, A. M. Winer, *Int. J. Chem. Kinet.*, **20**, 273 (1988).
- M. A. Goodman, S. M. Aschmann, R. Atkinson, A. M. Winer, *Arch. Environ. Contam. Toxicol.*, **17**, 281 (1988).
- M. A. Goodman, S. M. Aschmann, R. Atkinson, A. M. Winer, *Environ. Sci. Technol.*, **22**, 578 (1988).
- R. Atkinson, J. Arey, *Chem. Rev.*, **103**, 4605 (2003).
- S. M. Aschmann, E. C. Tuazon, R. Atkinson, *J. Phys. Chem. A*, **109**, 11828 (2005).
- S. M. Aschmann, E. C. Tuazon, R. Atkinson, *J. Phys. Chem. A*, **109**, 2282 (2005).
- S. M. Aschmann, R. Atkinson, *J. Phys. Chem. A*, **110**, 13029 (2006).
- S. M. Aschmann, E. C. Tuazon, W. D. Long, R. Atkinson, *J. Phys. Chem. A*, **114**, 3523 (2010).
- B. Eren, Y. Yalçın Gürkan, *JSCS.*, **82** (3), 277 (2017).
- I. Losito, A. Amorisco, F. Palmisano, *Journal of Chromatography A*, **1187** (1-2), 145 (2008).
- M. A. Oturan, J. J. Aaron, *Crit. Rev. Environ. Sci. Technol.*, **44**, 2577 (2014).
- Y. S. Wu, C. C. Chen, Y. C. Huang, W. Y. Lin, Y. T. Yen, C. S. Lu, *Sep. Sci. Technol.*, **51**, 2284 (2016).
- Y. Wang, H. Zhao, J. Gao, G. Zhao, Y. Zhang, *Phys. Chem. C*, **116**, 7457 (2012).
- X. Chen, S. S. Mao, *Chem. Rev.*, **107**, 2891 (2007).
- M. Sturini, E. Fasani, C. Prandi, A. Casaschi, A. Albini, *J. Photochem. Photobiol. A: Chem.*, **101**, 251 (1996).

18. H. F. Lai, C. C. Chen, R. J. Wu, C. S. Lu, *J. Chin. Chem. Soc.*, **59**, 87 (2012).
19. Y. Yalçın Gürkan, E. Kasapbaşı, Z. Çınar, *Chemical Engineering Journal*, **214**, 34 (2013).
20. <http://www.drugbank.ca/drugs/DB11.448>.
21. <http://extoxnet.orst.edu/pips/phosmet.htm>.
22. <https://www.ncbi.nlm.nih.gov/mesh/68.010.706>.
23. M. J. O'Neil, *The Merck Index - An Encyclopedia of Chemicals, Drugs, and Biologicals*. (13th ed.), Whitehouse Station, NJ: Merck and Co. Inc., 2001, p.1315.
24. C. D. S. Tomlin, Phosmet (732-11-6), in: *The e-Pesticide Manual*. (13th ed.), UK, British Crop Protection Council, 2004-05.
25. G. D. Clayton, F. E. Clayton, *Patty's Industrial Hygiene and Toxicology* (3rd ed.), New York, John Wiley & Sons, 2A, 2B, 2C, 1981, p. 4822.
26. D. Hartley, H. Kidd, *The Agrochemicals Handbook*. (2nd ed.), Lechworth, Herts, England, The Royal Society of Chemistry A., 1987, p. 325.
27. R. J. Lewis, *Sax's Dangerous Properties of Industrial Materials* (9th ed.), NY, Van Nostrand Reinhold, 1-3, 1996b, p. 2698. D. Hartley, H. Kidd, *The Agrochemicals Handbook*, (2nd ed.), Lechworth, Herts, England, The Royal Society of Chemistry A. 1987, p. 325.
28. Gaussian 09, Revision B.04, Gaussian Inc., Pittsburgh, PA, 2009